

Automatic calibration method of voxel size for cone-beam 3D-CT scanning system*

YANG Min(杨民)¹ WANG Xiao-Long(王晓龙)¹ LIU Yi-Peng(刘义鹏)² MENG Fan-Yong(孟凡勇)³
LI Xing-Dong(李兴东)⁴ LIU Wen-Li(刘文丽)⁴ WEI Dong-Bo(魏东波)¹

¹ School of Mechanical Engineering and Automation, Beijing Univ. of Aeronautics and Astronautics, Beijing 100191, China

² Department of Control Science and Engineering, Harbin Institute of Technology, Harbin 150001, China

³ State Key Laboratory of Multiphase Complex Systems, Institute of Process Engineering, Chinese Academy of Sciences, Beijing 100190, China

⁴ National Institute of Metrology, Beijing 100013, China

Abstract: For a cone-beam three-dimensional computed tomography (3D-CT) scanning system, voxel size is an important indicator to guarantee the accuracy of data analysis and feature measurement based on 3D-CT images. Meanwhile, the voxel size changes with the movement of the rotary stage along X-ray direction. In order to realize the automatic calibration of the voxel size, a new and easily-implemented method is proposed. According to this method, several projections of a spherical phantom are captured at different imaging positions and the corresponding voxel size values are calculated by non-linear least-square fitting. Through these interpolation values, a linear equation is obtained that reflects the relationship between the voxel size and the rotary stage translation distance from its nominal zero position. Finally, the linear equation is imported into the calibration module of the 3D-CT scanning system. When the rotary stage is moving along X-ray direction, the accurate value of the voxel size is dynamically exported. The experimental results prove that this method meets the requirements of the actual CT scanning system, and has virtues of easy implementation and high accuracy.

Key words: cone-beam CT, voxel size, least square fitting, automatic calibration

PACS: 87.59.bd **DOI:** 10.1088/1674-1137/38/4/046202

1 Introduction

With the rapid development of computer technology and the wide use of flat panel detectors, three-dimensional CT (3D-CT) has recently generated intense interest from both scientific studies and practical applications in the non-destructive testing (NDT) field [1, 2]. 3D reconstruction is carried out to get the internal structure and density distribution of the tested object through DR projection sequences collected by the detector at different imaging views during the rotation of the tested object [3–6]. As one important step of 3D-CT, back projection addresses are calculated in the image geometry coordinate system with the unit of a pixel, so the reconstructed data can not reflect the actual size of the tested object directly. For 3D-CT reconstruction, the tested object is considered as a virtual cuboid consisting of a large number of small cubes with a certain size stacking together regularly. These small cubes are named as voxels

and their actual physical size is called voxel size, which is an important indicator to describe the resolution of the cone-beam 3D-CT scanning system. A smaller voxel size indicates a higher spatial resolution of a 3D image. The accurate value of the voxel size also guarantees the accuracy of data analysis and feature measurement based on 3D-CT images [7, 8]. However, 3D reconstruction is realized in image geometry coordinate system with the unit of pixel, so the original voxel size must be in pixel unit. Accordingly, after the reconstruction, translating the original voxel size with pixel unit to the actual physical voxel size is a necessary step among the calibration of the cone beam 3D-CT scanning system. Furthermore, during CT scanning, when the tested object is placed in different positions between the X-ray source and the flat panel detector, the voxel size will be changed correspondingly. Therefore, we need to dynamically calibrate the voxel size complying with the variation of geometrical magnification ratio (GMR) caused by the alteration of

Received 8 May 2013

* Supported by National Natural Science Foundation of China (NSFC) (11275019, 21106158, 61077011), National State Key Laboratory of Multiphase Complex Systems (MPCS-2011-D-03), National Key Technology R&D Program of China (2011BAI02B02), Beijing Municipal Commission of Education (BMCE) Under the Joint-Building Project and National Key Scientific Apparatus Development of Special Item of China (2013YQ240803)

©2014 Chinese Physical Society and the Institute of High Energy Physics of the Chinese Academy of Sciences and the Institute of Modern Physics of the Chinese Academy of Sciences and IOP Publishing Ltd

the tested object's imaging position. The existing calibration methods need a special phantom to be scanned first, then the corresponding GMR and voxel size are calibrated. These methods are complicated and time-consuming because when the GMR changes the phantom has to be scanned again [9, 10]. Here, we propose a new easily-implemented method to calibrate voxel size. According to this method, several projections of a spherical phantom are captured in different imaging positions along X-ray direction and the corresponding voxel size values are calculated by non-linear least square fitting. Through these interpolation values, a linear equation is obtained that reflects the relationship between the voxel size and the rotary stage translation distance from its nominal zero position, so as to realize dynamic calibration of the voxel size. The experimental results prove that this method meets the requirements of the actual CT scanning system and has the virtues of easy implementation and high accuracy.

2 Methods

The principle of a cone-beam 3D-CT scanning system is shown in Fig. 1. The cone-beam X-ray penetrates the tested object fixed on the rotary stage and reaches the flat panel detector. The tested object rotates with a certain angle step at the drive of the rotary stage. The flat panel detector collects DR projections of the tested object at different imaging views among 360°. With all DR projections, 3D reconstruction is performed and cross-sectional images are obtained. As shown in Fig. 1, the imaging coordinate system is $X_d Y_d Z_d$, where 3D reconstruction operation is performed with the unit of a pixel. When the position of the detector in the imaging system is fixed, the imaging coordinate system will be determined. The object coordinate system is XYZ where the actual size of the tested object lies. So, before the feature measurement and data analysis through 3D-CT images, mapping the coordinate system $X_d Y_d Z_d$ to XYZ is necessary, namely calculating the voxel size. Furthermore, when the tested object is moving between the X-ray source and the flat panel detector, the value of the voxel size will be changed correspondingly, so the automatic calibration is also needed. For a 3D-CT scanning system, when the type of flat panel detector is determined, the physical size of the detection unit, namely the physical size of one pixel is constant, here we define the constant value as U . When one voxel unit in the tested object is projected to one pixel on the imaging plane of the detector, its projection size will be amplified by GMR times. Accordingly, the relationship between a voxel size and a detection unit size is:

$$V_i = U / M_i, \quad (1)$$

where M_i represents GMR at any imaging position, V_i is the voxel size at M_i imaging position. From the geometrical configuration in Fig. 2, GMR at any imaging position can be calculated as:

$$M_i = D_{\text{FOD}} / L_i, \quad (2)$$

where D_{FOD} is the distance from the X-ray focus to the imaging plane. When a 3D-CT scanning system is set up, the value of D_{FOD} will be constant and can be measured by multi-projection methods [11, 12]. L_i is the distance from the rotation center of the rotary stage to the X-ray focus, which cannot be measured directly. Obviously, $0 < L_i < D_{\text{FOD}}$. Therefore, the difficulty of the calibration of M_i is how to obtain the value of L_i in Eq. (2) quickly and accurately.

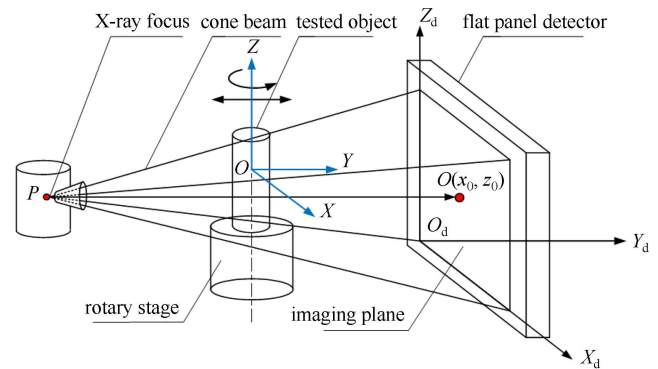


Fig. 1. The sketch of 3D-CT scanning ways.

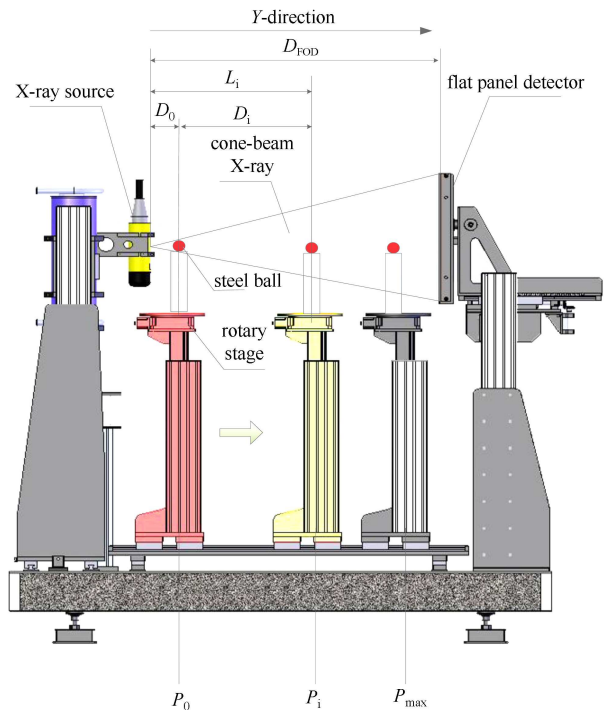


Fig. 2. (color online) The principle diagram of voxel size calibration.

From Fig. 2, L_i equals to

$$L_i = D_0 + D_i, \quad (3)$$

where D_0 is the distance from the nominal zero position (also starting position) of the rotary stage to the X-ray focus along Y-direction. The nominal zero position of the rotary stage at Y-direction is P_0 , which is designed well in advance according to the system movement control requirements. Thus, after the 3D-CT scanning system is assembled, D_0 is also a constant value, which unfortunately cannot be accurately measured. When the rotary stage moves to P_i position within the movement range along Y-direction, its translating distance from the starting position P_0 can be accurately recorded by the motor controller, here we define the distance as D_i . Combining Eqs. (1), (2) and (3), we have:

$$V_i = U \frac{D_0}{D_{\text{FOD}}} + \frac{U}{D_{\text{FOD}}} D_i. \quad (4)$$

Let $b = U \frac{D_0}{D_{\text{FOD}}}$, $k = \frac{U}{D_{\text{FOD}}}$, obviously, b and k are constant values, then Eq. (4) becomes:

$$V_i = b + k D_i. \quad (5)$$

The general expression of the relationship between voxel size and movement distance of the rotary stage is:

$$V = b + k D, \quad (6)$$

where V represents the voxel size, and V_i represents a sampled value of V . D is the movement distance of the rotary stage along Y-direction and D_i represents a sampled value of D .

From Eq. (6), we can find that, if we get the accurate values of b and k , the automatic calibration of the voxel size is realized. Obviously, Eq. (6) is a linear equation, so the optimal way to get the accurate values of b and k is linear fitting. According to the linear fitting method, some discrete values of V and D should be known in advance. In the practical implementation, we use a spherical phantom to realize linear fitting. As shown in Fig. 2, first we get several DR (digital radiography) projections of the spherical phantom at different imaging positions along Y-direction, where the corresponding moving distances are recorded by the motor controller, named as $[D_1, D_2, \dots, D_n]$. The projection is in a circular shape. Then, the image segmentation, edge

detection, image thinning and moment match tracing are applied to each circular projection to obtain one closed circle contour of the projection [13, 14]. During this step, a sub-pixel accuracy edge tracing method is applied to obtain the contour points (as shown in Fig. 3), which is realized by two kinds of edge detection algorithms. First, the pixel-level detection by Canny operator is adopted, which has single-pixel response and good performance for improving the signal-to-noise ratio and location accuracy. Then, the moment match tracing algorithm is employed based on the Canny-tracing results. The coordinates of the contour points with sub-pixel accuracy are acquired by solving the equations derived by an assumption that the ideal mixed moment is equal to the actual mixed moment of the image [15]. Based on the coordinates of contour points, the least-square fitting algorithm is used to calculate the diameter of the circular projection.

The equation of the fitted circle is given as:

$$(x - z_0)^2 + (z - z_0)^2 = r^2, \quad (7)$$

where (x_0, z_0) is the center of the fitted circle, r is the radius, and (x_i, z_i) is the contour point of the circular projection. The error function of the fitted circle can be expressed as:

$$E = \sum_{i=1}^n (x_i^2 - 2x_i x_0 + z_i^2 - 2z_i z_0 + k)^2, \quad (8)$$

where $k = x_0^2 + z_0^2 - r^2$

Let $\frac{\partial E}{\partial x_0} = 0$, $\frac{\partial E}{\partial z_0} = 0$, $\frac{\partial E}{\partial k} = 0$, then:

$$\begin{cases} \frac{\partial E}{\partial x_0} = 2 \sum_{i=1}^n (x_i^2 - 2x_i x_0 + z_i^2 - 2z_i z_0 + k)(-2x_i) = 0 \\ \frac{\partial E}{\partial z_0} = 2 \sum_{i=1}^n (x_i^2 - 2x_i x_0 + z_i^2 - 2z_i z_0 + k)(-2z_i) = 0 \\ \frac{\partial E}{\partial k} = 2 \sum_{i=1}^n (x_i^2 - 2x_i x_0 + z_i^2 - 2z_i z_0 + k) = 0 \end{cases}, \quad (9)$$

where n is the number of contour points. By solving the equations, the diameter value of each circular projection is obtained with the pixel unit. Here, we define the fitted diameter value as W'_i , so the corresponding voxel size value is obtained:

$$V_i = \frac{W}{W'_i}, \quad (10)$$

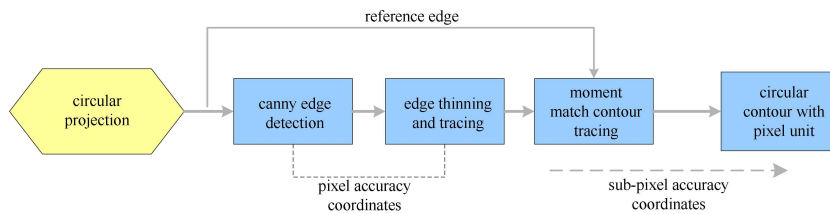


Fig. 3. Flow chart of an edge tracing method with sub-pixel accuracy.

where W is the actual diameter of the spherical phantom, which can be accurately measured by mechanical or photoelectrical means such as laser or coordinate measuring machine (CMM). By inputting the discrete values of V and D to Eq. (6), an equation set is gained:

$$\begin{bmatrix} D_1 & 1 \\ D_2 & 1 \\ \dots & 1 \\ D_i & 1 \\ \dots & 1 \\ D_n & 1 \end{bmatrix} \begin{bmatrix} k \\ b \end{bmatrix} = \begin{bmatrix} V_1 \\ V_2 \\ \dots \\ V_i \\ \dots \\ V_n \end{bmatrix}. \quad (11)$$

After solving the Eq. (11), the least-square solutions are b and k . Thereby, the expression of the Eq. (6) is reached. In line with the equation, as long as the translation distance of the rotary stage is imported, the corresponding voxel size is exported, which enables us to realize automatic calibration of the voxel size of the 3D-CT scanning system.

3 Results

In order to verify the effectiveness of the presented calibration method, we used a steel ball with diameter of 19 mm and fixed it on a support frame installed on the rotary stage of a micro 3D-CT scanning system. The micro-CT system employing micro-focus X-ray source and high-resolution flat-panel detector can provide micrometer-level spatial resolution. The main configuration parameters of the micro 3D-CT scanning system are:

Size of X-ray focus: 5 μm ; Size of imaging area: 200 mm \times 200 mm; Pixel size: 200 μm ; Source to Detector Distance (SDD): 695 mm.

In Eq. (9), we use the circle fitting to get the diameter of the projection. But actually, in the cone-beam radiation field, only when the center of the spherical phantom lies in the central X-ray will its projection be a circle, otherwise its projection will be an ellipse [12]. So, if we approximate the elliptical projection to a circle, then the final calibrating accuracy would be decreased theoretically. In our experiment, we moved the steel ball away from the central X-ray to make its projection drop in the marginal area of the imaging plane on the detector, and we then captured its projections at different GMR. We then adopted the elliptic non-linear least-square fitting to get the lengths of the major axis and the minor axis of each elliptical projection [16], and finally calculated its ellipticity (the ratio between the major axis and the minor axis), as shown in Fig. 4. From which we can find that, under the imaging geometrical configuration of the 3D-CT scanning system, the projection of a spherical phantom at any position in a cone-beam field is so close

to a circle that the error of the approximate circle fitting can be ignored. In the experiment, we first adjusted the steel ball's position to make sure that its projection was located in the central region of the imaging plane, where the rotary stage lied in the origin of XOZ -plane, namely $X=0$ mm and $Z=0$ mm. Then, we moved the rotary stage to the nominal zero position P_0 along Y -direction and captured a projection of the steel ball. We averaged 64 frames to one frame so as to increase the SNR (Signal to Noise Ratio) of the projection image. Next, the rotary stage was translated to its maximum distance position P_{max} along Y -direction and another projection of the steel ball was captured. Then, the rotary stage was moved to different positions between P_0 and P_{max} and several DR projections of the steel ball were acquired. After this, the image segmentation, edge detection, image thinning and moment match tracing were applied to each circular projection to obtain one closed circle contour. According to the coordinates of the contours, the non-linear least-square fitting method was employed to get the diameter of each circular projection in pixel units. The calculation results are shown in Table 1, where the maximum value of V_i is 94.4 μm and the minimum value is 28.4 μm . Meanwhile, we plotted a V_i - D_i graph, as shown in Fig.5, from which we can find that a satisfying linear relationship between translation distance of the rotary stage and the voxel size exists. In order to check the calibration accuracy when the steel ball's position varied along X and Z -direction, we repeated the above operation under the same GMR when the rotary stage was moved to the positions where $X=150$ mm, $Z=410$ mm and $X=-150$ mm, $Z=-300$ mm. In these two cases, the projection of the steel ball was close to the margin of the imaging plane. Fig. 6 shows one DR image of the steel ball and its edge contour after performing image processing when $D_i=330$ mm, $X=-150$ mm and $Z=-300$ mm. We can see that the projection has an ideal circular degree. After image processing and the non-linear least-square fitting, we plot the graphs of the two groups of V_i - D_i in Fig. 5, from which we can find that the three lines are almost same, which further validates that the final calibration result is not sensitive to the position variation of the steel ball along X or Z -direction. According to the three couples of the concrete values of V_i and D_i , the least-square solutions resulted in:

$$\begin{aligned} &X=0 \text{ mm}, Z=0 \text{ mm}: \\ &V=0.00028705D-0.03459384 \\ &X=150 \text{ mm}, Z=410 \text{ mm}: \\ &V=0.00028785D-0.03449271 \\ &X=-150 \text{ mm}, Z=-300 \text{ mm}: \\ &V=0.00029238D-0.03662287 \end{aligned}$$

By averaging the three linear equations, we got the final calibration equation:

$$V=0.00028909D-0.03523647. \quad (12)$$

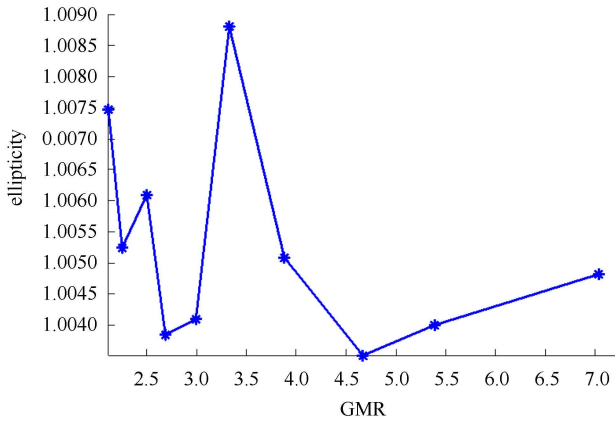


Fig. 4. The projection ellipticity statistics of a spherical phantom under different GMR.

Table 1. The measurement results of D_i-V_i .

D_i /mm	diameter W'_i (pixel)	GMR	voxel size V_i ($\times 10^{-2}$ mm)
220	668.65	7.038	2.84
250	512.25	5.392	3.71
270	443.52	4.669	4.28
300	368.75	3.882	5.15
330	316.16	3.328	6.01
350	284.28	2.992	6.68
380	255.32	2.688	7.44
400	237.10	2.496	8.01
430	214.23	2.255	8.87
450	201.28	2.119	9.44

Finally, Eq. (12) was loaded into the calibration module of the 3D-CT scanning system to realize the automatic calibration of the voxel size.

In order to verify the accuracy of the proposed method, we scanned a standard phantom in the same 3D-CT scanning system, then loaded all the cross-sectional

images and the voxel size, which was calculated by the proposed method, into the 3D visualization and analysis software Mimics10 (Materialise, Belgium), as shown in Fig. 7. On the base of the virtual 3D model, we selected several typical dimension parameters indicated in Fig. 7 and measured their value by the software. Table 2 gives the measurement results. We also measured the typical dimension parameters by CMM with much higher measurement precision [17]. The type of the CMM we used is PEARL1066/CP-8 and its measurement accuracy is 2.0 μm . By comparing the two kinds of measurement results, we can find that the proposed method here provides a voxel size with high precision, which ensures that the image analysis and feature measurement are more accurate and credible.

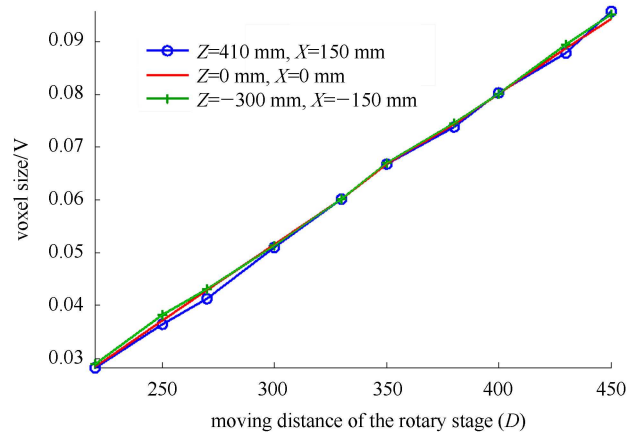


Fig. 5. Relationship diagram of D_i-V_i .

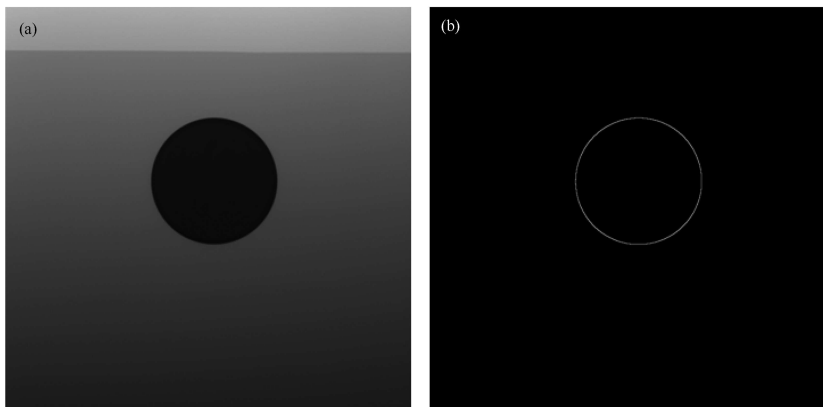


Fig. 6. DR projection and contour of a steel ball.

Table 2. Size measurement results of a standard phantom.

measurement	CMM/mm	mimics/mm	absolute error/mm	relative error(%)
D_1	44.992	45.086	0.094	0.21
D_2	74.978	75.151	0.173	0.23
D_3	9.056	9.093	0.037	0.41
H	49.973	50.040	0.067	0.13

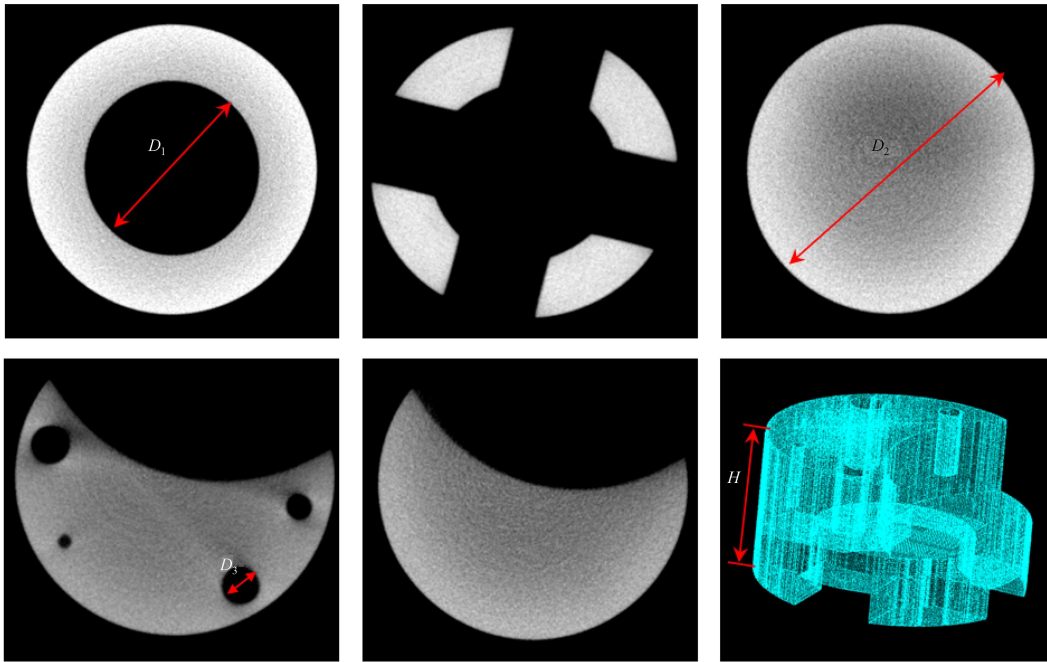


Fig. 7. CT slices and 3D virtual model of a standard phantom.

4 Conclusion

Voxel size is an important indicator to describe the resolution of a cone-beam 3D-CT scanning system. Its accuracy also guarantees the precision of data analysis and feature measurement based on 3D-CT images. In this paper, we proposed an automatic calibration method to get the voxel size with high precision. In line with this method, several circular projections of a spherical phantom are captured at different imaging positions along Y -direction, where the corresponding moving distances are recorded at the same time by a motor controller. Then, image segmentation, edge detection, image thinning and moment match tracing are applied to each circular pro-

jection to obtain one closed circle contour. Based on the coordinates of the contour points, least-square fitting is used to calculate the diameter of the circular projection. Through these interpolation values, a linear equation is obtained that reflects the relationship between the voxel size and the rotary stage translation distance from its nominal zero position. This linear equation is finally imported into the calibrating module of the 3D-CT scanning system. When the rotary stage moves along Y -direction, an accurate value of the voxel size is dynamically exported. The experimental results prove that this method meets the requirements of the actual 3D-CT scanning system and has the virtues of easy implementation and high accuracy.

References

- 1 Erik L, Ritman. *Annu. Rev. Biomed. Eng.*, 2004, **6**: 185–208
- 2 Lee Sang Chul, Kim Ho Kyung, Chun In Kon et al. *Phys. Med. Biol.*, 2003, **48**: 4173–4185
- 3 Altunbas M, Shaw C, Chen L. *Medical Physics*, 2006, **33**: 2287–2295
- 4 Sidky E Y, PAN X. *Phys. Med. Biol.*, 2008, **53**: 4777–4807
- 5 CHEN G H, TANG J, LENG S. *Med. Phys.*, 2008, **35**: 660–663
- 6 PAN X, Sidky E Y, Vannier M. *Inverse Probl.*, 2009, **25**: 123009
- 7 Nagarkar V V, Gordon J S, Vasile S et al. *IEEE Trans. on Nucl. Sci.*, 1996, **43**: 1559–1563
- 8 Maret D, Telmon N, Peters O A. *Dento maxillo facial radiology*, 2012, **41**: 649–655
- 9 Tanimoto H, Ara Y. *Oral Radiology*, 2009, **25**: 149–153
- 10 Bechara Boulos, McMahan C Alex, Moore William S. *Oral Surgery SURGERY Oral Medicine Oral Pathology Oral Radiology*, 2012, **214**: 658–665
- 11 YANG Min, GAO Haidong, LI Xing-Dong et al. *NDT&E International*, 2012, **46**: 48–54
- 12 YANG Min, JIN Xu-Ling, LI Bao-Lei. *Chin. Phys. C (HEP & NP)*. 2010, **34**: 1665–1670
- 13 Antoni Buades, Bartomeu Coll, Jean-Michel Morel. *Int. J. Comput. Vis.*, 2008, **76**: 123–139
- 14 YANG Min, YANG Yi-Min, WANG Chang-Sui. *Science and Technology*, 2011, **19**: 333–343
- 15 Lyvers E P, Mitchell O R. *IEEE Tans. on Pattern Analysis and Machine Intelligence*, 1989, **11**: 1293–1308
- 16 YAN Bei, WANG Bin, LI Yuan. *Journal of Beijing University of Aeronautics and Astronautics*, 2008, **34**: 295–298 (in Chinese)
- 17 Ryniewicz A, Accuray. *Metrol. Meas. Syst.*, 2010, **17**: 382–386